THE JOURNAL OF BIOLOGICAL CHEMISTRY
Vol. 279, No. 20, Issue of May 14, pp. 21271–21281, 2004

Printed in U.S.A.

The Deubiquitinating Enzyme Doa4p Protects Cells from DNA Topoisomerase I Poisons*

Received for publication, November 11, 2003, and in revised form, February 24, 2004
Published, JBC Papers in Press, February 26, 2004, DOI 10.1074/jbc.M312338200

Paola Fiorani‡§, Robert J. D. Reid¶‖, Antonino Schepis‡‡, Hervé R. Jacquiau‡, Hong Guo‡, Padma Thimmaiah‡, Piero Benedetti**§§, and Mary-Ann Bjornsti‡¶ ¶¶**

*From the ‡Department of Molecular Pharmacology, St. Jude Children's Research Hospital, Memphis, Tennessee 38105, the ¶Department of Biochemistry and Molecular Pharmacology, Thomas Jefferson University, Philadelphia, Pennsylvania 19107, **Institute of Cell Biology, CNR, Monterotondo, Italy, and the §§Department of Biology, University of Padua, 35131 Padua, Italy*

DNA topoisomerase I (Top1p) catalyzes changes in DNA topology via the formation of an enzyme-DNA covalent complex that is reversibly stabilized by the antitumor drug, camptothecin (CPT). During S-phase, collisions with replication forks convert these complexes into cytotoxic DNA lesions that trigger cell cycle arrest and cell death. To investigate cellular responses to CPT-induced DNA damage, a yeast genetic screen identified conditional *tah* mutants with enhanced sensitivity to self-poisoning DNA topoisomerase I mutant (Top1T722Ap), which mimics the action of CPT. Mutant alleles of three genes, *DOA4*, *SLA1* and *SLA2*, were recovered. A nonsense mutation in *DOA4* eliminated the catalytic residues of the Doa4p deubiquitinating enzyme, yet retained the rhodanase domain. At 36 °C, this *doa4-10* mutant exhibited increased sensitivity to CPT, osmotic stress, and hydroxyurea, and a reversible petite phenotype. However, the accumulation of pre-vacuolar class E vesicles that was observed in *doa4*Δ cells was not detected in the *doa4-10* mutant. Mutations in *SLA1* or *SLA2*, which alter actin cytoskeleton architecture, induced a conditional synthetic lethal phenotype in combination with *doa4-10* in the absence of DNA damage. Here actin cytoskeleton defects coincided with the enhanced fragility of large-budded cells. In contrast, the enhanced sensitivity of *doa4-10* mutant cells to Top1T722Ap was unrelated to alterations in endocytosis and was selectively suppressed by increased dosage of the ribonucleotide reductase inhibitor Sml1p. Additional studies suggest a role for Doa4p in the Rad9p checkpoint response to Top1p poisons. These findings indicate a functional link between ubiquitin-mediated proteolysis and cellular resistance to CPT-induced DNA damage.

DNA topoisomerases catalyze changes in the linkage of DNA strands, allowing for DNA unwinding or decatenation during DNA replication, transcription, recombination, and chromosome segregation (1, 2). Eukaryotic DNA topoisomerase I (Top1p) transiently cleaves a single strand of duplex DNA and forms a covalent tyrosyl linkage with a 3′-phosphoryl DNA end. The covalent Top1p-DNA intermediate allows for DNA rotation while conserving the energy of the cleaved phosphodiester bond.

DNA topoisomerase I is the cellular target of the antitumor drug, camptothecin (CPT),[1] which reversibly stabilizes the covalent Top1p-DNA complex by inhibiting DNA religation (3–5). The ternary CPT-Top1p-DNA complexes *per se* are insufficient to induce a cytotoxic response. Rather, collisions with advancing replication forks convert the drug-stabilized complexes into the irreversible DNA lesions that trigger cell cycle arrest and cell death. This model is consistent with the S-phase specificity of CPT and the observation that inhibition of DNA synthesis by aphidicolin abrogates the cytotoxic action of the drug (6).

In the yeast *Saccharomyces cerevisiae*, DNA topoisomerase I is nonessential (6, 7). *top1*Δ strains are resistant to CPT, although drug sensitivity may be restored by expressing plasmid-borne yeast or human *TOP1*. Thus, the cytotoxic action of CPT does not derive from the inhibition of Top1p catalytic activity; rather the drug converts this nonessential enzyme into a cellular toxin.

Biochemical and structural data have begun to reveal the domainal organization of Top1p critical for DNA binding, enzyme catalysis, and CPT sensitivity (8–12). Single amino acid substitutions in Top1p have also been defined that alter enzyme sensitivity to CPT and other Top1p poisons or that alter the DNA cleavage-religation equilibrium of the enzyme in the absence of drug (13–25). In yeast Top1T722Ap, substitution of Ala for Thr-722 (five residues N-terminal to the active site tyrosine, Tyr-727) mimics the action of CPT by reducing the rate of DNA religation (26, 27). Similar effects on human enzyme activity were obtained with the same substitution at the corresponding position in hTop1T718Ap (24). These studies highlight the similarities in eukaryotic Top1p mechanism, structure, and sensitivity to CPT.

Considerably less is known of the cellular processes that regulate cellular responses to drug- or *top1* mutation-induced DNA lesions. Rad9p, Mec1p, and Rad53p checkpoints modulate cell sensitivity to CPT, consistent with studies in mammalian

* This work was supported by National Institutes of Health Grants CA58755 and CA70406 (to M.-A. B.), Ministero dell'Instruzione, dell'Università e della Ricerca Cofinanziamento 2001, Associazione Italiana per la Ricerca Sul Cancro, FIRB, Ministero della Salute and Genomica Funzionale CNR (to P. B.), a fellowship from the FIRC (to P. F.), NCI Cancer Center Core Grant CA21765 from the National Institutes of Health, and American Lebanese Syrian Associated Charities. The costs of publication of this article were defrayed in part by the payment of page charges. This article must therefore be hereby marked "*advertisement*" in accordance with 18 U.S.C. Section 1734 solely to indicate this fact.

§ Present address: Dept. of Biology, University of Rome Tor Vergata, 00133 Rome, Italy.

‖ Present address: Dept. of Genetics and Development, Columbia University, College of Physicians and Surgeons, New York, NY 10032.

‡‡ Present address: EMBL Heidelberg, D-69117 Heidelberg, Germany.

¶¶ To whom correspondence should be addressed: Dept. of Molecular Pharmacology, St. Jude Children's Research Hospital, 332 N. Lauderdale, Memphis, TN 38105. Tel.: 901-495-2315; Fax: 901-495-4290; E-mail: Mary-Ann.Bjornsti@stjude.org.

[1] The abbreviations used are: CPT, camptothecin; ts, temperature-sensitive; HU, hydroxyurea; DAPI, 4,6-diamidino-2-phenylindole; DUB, deubiquitinating enzyme; FOA, fluoroorotic acid; DIC, differential interference contrast.

TABLE I
Yeast strains

Strain	Genotype	Ref.
EKY2	*MAT***a**, *ura3-52*, *his3Δ200*, *leu2Δ1*, *trp1Δ63*, *top1Δ::HIS3*	56
EKY3	*MAT***a**, *ura3-52*, *his3Δ200*, *leu2Δ1*, *trp1Δ63*, *top1Δ::TRP1*	56
RRY72-3	*MAT***a**, *ura3-52*, *his3Δ200*, *leu2Δ1*, *trp1Δ63*, *top1Δ::TRP1*, *cdc45–10*	39
RRY76-3	*MAT***a**, *ura3-52*, *his3Δ200*, *leu2Δ1*, *trp1Δ63*, *top1Δ::TRP1*, *sla1-10*	This work
PFY83	*MAT***a**, *ura3-52*, *his3Δ200*, *leu2Δ1*, *trp1Δ63*, *top1Δ::TRP1*, *sla1-10*, rho^0	This work
RRY84-3	*MAT***a**, *ura3-52*, *his3Δ200*, *leu2Δ1*, *trp1Δ63*, *top1Δ::TRP1*, *sla2-10*	This work
RRY90	*MAT***a**, *ura3-52*, *his3Δ200*, *leu2Δ1*, *trp1Δ63*, *top1Δ::TRP1*, *sla1-20*	This work
RRY92-3	*MAT***a**, *ura3-52*, *his3Δ200*, *leu2Δ1*, *trp1Δ63*, *top1Δ::TRP1*, *doa4-10*	This work
PFY52	*MAT***a**, *ura3-52*, *his3Δ200*, *leu2Δ1*, *trp1Δ63*, *top1Δ::TRP1*, *doa4-10*, rho^0	This work
MSY6	*MAT***a**, *ura3-52*, *his3Δ200*, *leu2Δ1*, *trp1Δ63*, *top1Δ::TRP1*, *doa4-10*, *cdc45–10*	This work
MSY61	*MAT***a**, *ura3-52*, *his3Δ200*, *leu2Δ1*, *trp1Δ63*, *top1Δ::TRP1*, *doa4-10*, *sla1-10*	This work
PFY84	*MAT***a**, *ura3-52*, *his3Δ200*, *leu2Δ1*, *trp1Δ63*, *top1Δ::TRP1*, *doa4-10*, *sla1-10*, rho^0	This work
MSY75	*MAT***a**, *ura3-52*, *his3Δ200*, *leu2Δ1*, *trp1Δ63*, *top1Δ::TRP1*, *doa4-10*, *sla2-10*	This work
MSY85	*MAT***a**, *ura3-52*, *his3Δ200*, *leu2Δ1*, *trp1Δ63*, *top1Δ::TRP1*, *doa4Δ::URA3*	This work
PFY53	*MAT***a**, *ura3-52*, *his3Δ200*, *leu2Δ1*, *trp1Δ63*, *top1Δ::TRP1*, *doa4Δ::URA3*, rho^0	This work
MMY3	*MAT***a**, *ura3-52*, *his3Δ200*, *leu2Δ1*, *trp1Δ63*, *top1Δ::TRP1*, *rad9Δ::hisG*	26
PFY74	*MAT***a**, *ura3-52*, *his3Δ200*, *leu2Δ1*, *trp1Δ63*, *top1Δ::TRP1*, *doa4-10*, *rad9Δ::his5+*	This work
PFY50	*MAT***a**, *ura3-52*, *his3Δ200*, *leu2Δ1*, *trp1Δ63*, *top1Δ::TRP1*, *sml1Δ::his5+*	This work
PFY48	*MAT***a**, *ura3-52*, *his3Δ200*, *leu2Δ1*, *trp1Δ63*, *top1Δ::TRP1*, *doa4-10*, *sml1Δ::his5+*	This work
PFY68	*MAT***a**, *ura3-52*, *his3Δ200*, *leu2Δ1*, *trp1Δ63*, *top1Δ::TRP1*, *tdp1Δ::his5+*	This work
PFY67	*MAT***a**, *ura3-52*, *his3Δ200*, *leu2Δ1*, *trp1Δ63*, *top1Δ::TRP1*, *doa4-10*, *tdp1Δ::his5+*	This work
PFY60	*MAT***a**, *ura3-52*, *his3Δ200*, *leu2Δ1*, *trp1Δ63*, *top1Δ::TRP1*, *doa4-10*, *sla1Δ::his5+*	This work
PFY61	*MAT***a**, *ura3-52*, *his3Δ200*, *leu2Δ1*, *trp1Δ63*, *top1Δ::TRP1*, *doa4Δ::URA3*, *sla1Δ::his5+*	This work
PFY62	*MAT***a**, *ura3-52*, *his3Δ200*, *leu2Δ1*, *trp1Δ63*, *top1Δ::TRP1*, *sla1Δ::his5+*	This work
PFY73	*MAT***a**, *ura3-52*, *his3Δ200*, *leu2Δ1*, *trp1Δ63*, *top1Δ::TRP1*, *rad17Δ::his5+*	This work
PFY72	*MAT***a**, *ura3-52*, *his3Δ200*, *leu2Δ1*, *trp1Δ63*, *top1Δ::TRP1*, *doa4-10*, *rad17Δ::his5+*	This work
PFY81	*MAT***a**, *ura3-52*, *his3Δ200*, *leu2Δ1*, *trp1Δ63*, *top1Δ::TRP1*, *chk1Δ::his5+*	This work
PFY80	*MAT***a**, *ura3-52*, *his3Δ200*, *leu2Δ1*, *trp1Δ63*, *top1Δ::TRP1*, *doa4-10*, *chk1Δ::his5+*	This work
PFY90	*MAT***a**, *ura3-52*, *his3Δ200*, *leu2Δ1*, *trp1Δ63*, *top1Δ::TRP1*, *tof1Δ::his5+*	This work
PFY91	*MAT***a**, *ura3-52*, *his3Δ200*, *leu2Δ1*, *trp1Δ63*, *top1Δ::TRP1*, *doa4-10*, *tof1Δ::his5+*	This work
PTY15	*MAT***a**, *ura3-52*, *his3Δ200*, *leu2Δ1*, *trp1Δ63*, *top1Δ::TRP1*, *tel1Δ::his5+*	This work
PTY12	*MAT***a**, *ura3-52*, *his3Δ200*, *leu2Δ1*, *trp1Δ63*, *top1Δ::TRP1*, *doa4-10*, *tel1Δ::his5+*	This work
PTY4	*MAT***a**, *ura3-52*, *his3Δ200*, *leu2Δ1*, *trp1Δ63*, *top1Δ::TRP1*, *rad24Δ::his5+*	This work
PTY5	*MAT***a**, *ura3-52*, *his3Δ200*, *leu2Δ1*, *trp1Δ63*, *top1Δ::TRP1*, *doa4-10*, *rad24Δ::his5+*	This work
PFY79	*MAT***a**, *ura3-52*, *his3Δ200*, *leu2Δ1*, *trp1Δ63*, *top1Δ::TRP1*, *sml1Δ::HIS3*, *mec1Δ::KAN*	This work
PTY13	*MAT***a**, *ura3-52*, *his3Δ200*, *leu2Δ1*, *trp1Δ63*, *top1Δ::TRP1*, *doa4-10*, *sml1Δ::his5+*, *mec1Δ::KAN*	This work
PTY6	*MAT***a**, *ura3-52*, *his3Δ200*, *leu2Δ1*, *trp1Δ63*, *top1Δ::TRP1*, *sml1Δ::HIS3*, *rad53Δ::KAN*	This work
PTY14	*MAT***a**, *ura3-52*, *his3Δ200*, *leu2Δ1*, *trp1Δ63*, *top1Δ::TRP1*, *doa4-10*, *sml1Δ::his5+*, *rad53Δ::KAN*	This work
HJY6	*MAT***a**, *ura3-52*, *his3Δ200*, *leu2Δ1*, *trp1Δ63*, *top1Δ::TRP1*, *DOA4*-HA	This work
HJY7	*MAT***a**, *ura3-52*, *his3Δ200*, *leu2Δ1*, *trp1Δ63*, *top1Δ::TRP1*, *doa4-10*-HA	This work
HGY1	*MAT***a**, *ura3-52*, *his3Δ200*, *leu2Δ1*, *trp1Δ63*, *top1Δ::TRP1*, *vps4Δ::his5+*	This work
HGY2	*MAT***a**, *ura3-52*, *his3Δ200*, *leu2Δ1*, *trp1Δ63*, *top1Δ::TRP1*, *doa4-10*, *vps4Δ::his5+*	This work
PTY44	*MAT***a**, *ura3-52*, *his3Δ200*, *leu2Δ1*, *trp1Δ63*, *top1Δ::TRP1*, *ubp5Δ::his5+*	This work
LBY11	*MAT***a**, *ura3-52*, *his3Δ200*, *leu2Δ1*, *trp1Δ63*, *top1Δ::TRP1*, *ubp11Δ::TRP1*	This work
PTY43	*MAT***a**, *ura3-52*, *his3Δ200*, *leu2Δ1*, *trp1Δ63*, *top1Δ::TRP1*, *ubp12Δ::his5+*	This work

cells demonstrating the activation of the ATR/CHK1 checkpoint in response to drug treatment (26, 28–34). Rad9p also protects cells from self-poisoning *top1* mutants, including Top1T722Ap (26). The induction of double-stranded DNA breaks has, in part, been inferred by the enhanced sensitivity of *rad52*Δ strains to Top1p-DNA lesions (35). More direct evidence for alterations in DNA replication potentiating the cytotoxic action of CPT comes from studies demonstrating the enhanced drug sensitivity of yeast strains mutated for *SGS1*, *MUS81*, *TRF4*, *CDC45*, and *DPB11* (29, 30, 36–40). In the case of the Sgs1 helicase or Mus81p, alterations in fork regression might preclude repair of Top1-DNA lesions (36–38). Trf4p (DNA polymerase σ) activity is required to establish sister chromatid cohesion and for *top1*Δ cell viability (40). Hypomorphic alleles of *CDC45* and *DBP11*, isolated in our screen for top1T722A- hypersensitive (*tah*) mutants, induce a transient accumulation of Okazaki-sized DNA fragments and enhance cell sensitivity to Top1p-induced DNA damage (39). These results link processive DNA replication with cellular resistance to CPT.

Here we report the characterization of three additional *tah* mutants, *doa4-10*, *sla1-10,* and *sla2-10*, that exhibit enhanced sensitivity to the self-poisoning Top1T722Ap at 36 °C. We provide evidence that the Doa4 deubiquitinating enzyme and the cortical actin proteins, Sla1p and Sla2p, function to protect cells from Top1p-induced DNA damage. Doa4p is a ubiquitin-specific protease that physically associates with the 26 S proteasome and recycles ubiquitin from proteins targeted for proteolytic degradation (41, 42). Doa4p also functions in the endocytic pathway to remove ubiquitin from plasma membrane proteins targeted for vacuolar degradation (43). Sla1p and Sla2p function in the assembly of cortical actin patches and the actin cytoskeleton (44, 45) and in endocytosis (46).

We also report that the ribonucleotide reductase inhibitor, Sml1p (47), functions as a specific dosage suppressor of *doa4-10* sensitivity to Top1T722Ap-induced lethality. Further studies of checkpoint mutants, such as *rad9*Δ, *mec1*Δ, and *tel1*Δ, suggest *doa4-10*-mediated alterations in the Rad9p DNA damage checkpoint. These results are discussed in terms of a functional link between ubiquitin-mediated proteolysis, cortical actin organization, and cellular responses to Top1p poisons.

EXPERIMENTAL PROCEDURES

Strains and Plasmids—Yeast strains are listed in Table I. Gene disruptions were made by PCR (48). *ARS*/*CEN* vectors expressing *TOP1* and *top1T722A* from constitutive *TOP1* promoters, YCpScTOP1 and YCpSctop1T722A, respectively, were described (26). Analogous *LEU2*-based vectors, YCpScTOP1·L or YCp-Sctop1T722A·L, were constructed by ligating an ApaI/SacII DNA fragment into plasmid pRS415. pRS416 and pRS415 served as vector controls (49). The *URA3*, *ARS*/*CEN* plasmid-based yeast genomic DNA library, YCp-FY250, was described

(39). A YEp-FY250 yeast genomic DNA library was similarly constructed by ligating size-fractionated (6–10 kbp) and partially Sau3A-digested DNA into the dephosphorylated BamHI ends of vector YEp24-PL, followed by amplification in *Escherichia coli*.

tah Mutant Isolation—A genetic screen for *tah* mutants exhibiting temperature sensitivity to *top1T722A* was described (39). Briefly, *top1*Δ cells, transformed with YCpSctop1T722A, were subjected to ethyl methonesulfonate mutagenesis and screened for colonies exhibiting temperature-sensitive (ts) growth at 36 °C. Plating on 5-FOA eliminated mutants where ts growth was not linked to plasmid-encoded Top1T722Ap. Backcrossing to *TAH+, top1*Δ strains identified 10 *tah* mutants, where a single recessive gene defect was linked to *top1T722A* hypersensitivity. Complementation analysis determined that *tah6* and *tah20* were allelic.

Cloning DOA4, SLA1, and SLA2 by Complementation—*tah22*, *tah20*, and *tah14* strains, transformed with YCp-FY250 library DNA, were screened for plasmid-dependent growth at 36 °C on SC-uracil media containing 10 mg/ml HU. The smaller of the overlapping *TAH22* clones contained 5.9 kbp of chromosome IV including *YDR068*, *DOA4*, and *YDR070*. A *TAH20* clone contained 5.7 kbp of chromosome II encompassing *SLA1* and *YBL006*. This clone also complemented the HU hypersensitivity of the *tah6* strain. *TAH14* clone contained 8.4 kbp of chromosome XIV with only one gene, *SLA2*. Subcloning confirmed that *DOA4*, *SLA1*, and *SLA2* complemented the HU and *top1T722A* hypersensitivity of *tah22*, *tah6*/*tah20*, and *tah14*, respectively. A YEpDOA4 vector was made by ligating a 5.4-kbp SpeI DNA fragment, excised from *TAH22* clone, into YEp24-PL.

To confirm the genetic identity of *TAH22* as *DOA4*, *TAH6/20* as *SLA1*, and *TAH14* as *SLA2*, a selectable *URA3* (or *LEU2*) marker was integrated into the genomic sequences flanking *DOA4*, *SLA1*, and *SLA2*, respectively. After mating with respective *tah22*, *tah6*, and *tah14* mutants, meiotic products were assessed for segregation of uracil (or leucine) prototrophy and the *tah* phenotype. Integration constructs were as follows: a 2.7-kbp NotI DNA fragment from *TAH22* clone was ligated into pRS406 to yield YIpDOA4·U or pRS405 to make YIpDOA4·L. Transformation of EKY2 cells with MscI-digested DNA targeted integration 5′ to *DOA4*. A LEU2-based YIpSLA1·L vector was made by ligating a 2.1-kbp PstI DNA fragment from *TAH20* clone, into pRS405. AvrII digestion targeted *URA3* integration 3′ to *SLA1*. To target *URA3* integration to sequences 3′ to *SLA2*, a 2.4-kbp NotI/XbaI DNA fragment excised from the *TAH14* clone was ligated into pRS406. EKY2 cells were transformed with HpaI-digested YIpSLA2.

Mutant *doa4-10* and *sla1-10* alleles were recovered after targeted integration of YIpDOA4·L and YIpSLA1·L, respectively. Purified genomic DNA was restricted with HindIII (*doa4-10*) or ClaI (*sla1-10*). Size-selected DNA fragments were ligated and transformed into *E. coli*. DNA sequencing defined the mutations in *doa4-10* and *sla1-10*.

A C-terminal HA tag was introduced into wild type *DOA4* using a *URA3* marker flanked by 3× HA tags (50). A C-terminal HA tag and stop codon were introduced after residue 387 in *DOA4* to generate *doa4-10-HA*. HA-*URA3*-HA was integrated into a single *DOA4* locus in diploid EKY23 cells. Meiotic products were screened for uracil prototrophy and sensitivity to HU. Excision of *URA3* was selected on 5-FOA plates, and the generation of *doa4-10-HA* was confirmed by DNA sequencing. *DOA4-HA* and *doa4-10-HA* cell sensitivity to *top1T722A*, CPT, and HU was indistinguishable from that of *DOA4* and *doa4-10* strains, respectively.

Cell Viability Assays—Exponentially growing cells, transformed with YCpScTOP1, YCpSctop1T722A, or pRS416, were 10-fold serially diluted, and 5-μl aliquots were spotted on SC-uracil plates. Cell viability was assessed after incubation at 26 °C or 36 °C. To assay CPT sensitivity, YCpScTOP1-transformed cells were spotted onto SC-uracil media plus 25 mM HEPES, pH 7.2, 0.125% Me_2SO and 0 or 5 μg/ml CPT. To quantitate colony formation, serial dilutions of transformed cells were plated onto SC-uracil media (+ or − CPT) and incubated at 26 or 36 °C. Cell sensitivity to methyl methanesulfonate (0.0125 or 0.025%), HU (5 or 10 mg/ml), or UV (10 or 20 μJ/M^2) was assayed as described (39). Sensitivity to high salt was assayed on YPD, 6% NaCl plates. Cell growth on nonfermentable carbon sources was assessed on yeast extract, peptone, 3% glycerol plates.

To quantitate HU sensitivity, cultures exponentially growing at 26 °C were divided, and half was treated with 15 mg/ml HU. After 30 min, the cultures were shifted to 36 °C ($t = 0$). At various times, aliquots were diluted and plated onto YPD media at 26 °C. Colony formation was assessed at 26 °C. Aliquots of cells were fixed with 70% ethanol and stored at −20 °C for subsequent DAPI staining and microscopy.

Actin Localization and DAPI Staining—Exponentially growing *DOA4*, *doa4-10*, and *sla1-10* cells, in YPD at 26 and 36 °C, were fixed with 3.7% formaldehyde. After 2 h, the pelleted cells were washed with phosphate-buffered saline. For actin staining (51), cells were resuspended in phosphate-buffered saline, stained with 0.66 μM rhodamine-phalloidin (Molecular Probes), and then mixed with mounting media (Molecular Probes) on polylysine-coated Teflon slides. For DAPI staining of DNA, cells spotted on polylysine-coated Teflon slides were suspended in 0.2 μg/ml DAPI and mounting media. Cells were viewed with a Zeiss Axioskop 2 microscope equipped with DIC, epifluorescence, and UV blocking filter sets. Images were acquired with a Micromax CCD camera and IP lab software (Scanalytics).

Electron Microscopy—Cells were fixed, embedded, and stained as described (52–55). Briefly, cells grown at 26 °C were divided, and half was shifted to 36 °C for 10 h. Cells, pelleted by centrifugation, were resuspended in freshly prepared 40 mM sodium phosphate, pH 6.7, 1 M sorbitol, 0.5% glutaraldehyde, and 3% formaldehyde for 1 h, washed three times with 40 mM sodium phosphate, pH 6.7, and resuspended in 1% $NaIO_4$ for 10 min. After quenching free aldehyde groups with 50 mM NH_4Cl, cells were washed with water and successively dehydrated in EtOH (50, 70, 80, 85, 90, and 95% and two washes in 100% EtOH) at 4 °C, followed by 100% EtOH at room temperature. Infiltration and polymerization of LR White embedding media were as per manufacturer's instructions (Polysciences). Thin sections (50 nm) were cut with a Leica UltraCut ultramicrotome, mounted on copper grids coated with a 2% collodium film, stained with 2% uranyl acetate and Reinold lead citrate, and observed in a Jeol Jem 10–10 microscope at 80 kV. Magnifications were corrected using a tropomyosin crystal standard.

DNA Topoisomerase I Activity and Immunoprecipitation—Top1 protein levels in *DOA4* and *doa4-10* cells transformed with YCpScTOP1 or YCpSctop1T722A were assessed in crude extracts prepared from exponential cultures grown at 26 °C or shifted to 36 °C for 4–24 h. As described (27), cells harvested by centrifugation were resuspended in 2 ml/g cells of TEEG buffer (20 mM Tris, pH 7.5, 10 mM EDTA, 10 mM EGTA, 10% glycerol) plus 0.2 M KCl and protease inhibitors and were stored at −80 °C. Thawed cells, lysed by vortexing with glass beads, were clarified by centrifugation. Extracts were also prepared from *DOA4* or *doa4-10* transformants replica-plated onto selective media and incubated at 26 or 36 °C for 24 or 48 h. Cells were collected and processed as described above. After correcting for total protein, DNA topoisomerase I catalytic activity was assessed in a plasmid DNA relaxation assay (14, 27). Top1p levels and integrity were assessed by SDS-PAGE and immunoblotting with a polyclonal antibody specific for yeast Top1p and chemiluminescence (Amersham Biosciences).

Extracts of exponentially growing *DOA4-HA* and *doa4-10-HA* cells, prepared as above, were immunoblotted with a monoclonal HA-specific antibody. Alternatively, cells were harvested by centrifugation and resuspended in SDS-PAGE sample buffer, and the proteins were resolved by SDS-PAGE. Although full-length Doa4p was readily detected, truncated Doa4-10-HA protein was sporadically observed at 36 °C. The inclusion of phosphatase inhibitors, *N*-ethylmaleimide, additional protease inhibitors, or osmotic stabilizers or extraction with high salt failed to enhance Doa4-10-HA stability.

Isolation of Dosage Suppressors—To isolate dosage suppressors, *doa4-10* cells, co-transformed with YCpSctop1T722A·L and YEp-FY250 DNA library, were incubated on SC-uracil, -leucine plates at 36 °C. To ensure that suppression of *doa4-10* cell sensitivity to *top1T722A* was linked to the YEp-FY250 vector, individual transformants were plated on SC-leucine, 5-FOA plates at 26 °C and re-screened for *top1T722A*-induced lethality at 36 °C. Transformants exhibiting YEp-FY250-dependent viability at 36 °C were selected and the YEp-DNAs isolated. Data base queries and subcloning of putative suppressors into YEp24-PL confirmed the identity of *UBI2*, *UBI4*, and *SML1* as dosage suppressors of *doa4-10*.

RESULTS

Doa4p, Sla1p, and Sla2p Affect Cell Sensitivity to DNA Topoisomerase I Poisons—To investigate cellular responses to Top1p poison-induced DNA lesions, a yeast genetic screen was performed to isolate ts mutants with enhanced sensitivity to CPT. To avoid issues of drug transport, a self-poisoning *top1T722A* mutant was used as a CPT mimetic. Although cytotoxic when overexpressed from p*GAL1* (26), low levels of Top1T722Ap are tolerated in repair-proficient, checkpoint-competent cells. On this basis, ts *tah* (Top1T722Ap-hypersensitive) mutants were isolated (39). We reported previously the alterations in processive DNA replication induced by two *tah* mutants, *cdc45-10* and *dpb11-10* (39). Here we report three

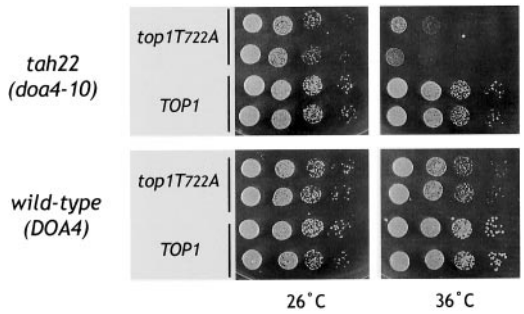

FIG. 1. ***tah22* (*doa4-10*) cells exhibit enhanced sensitivity to Top1T722Ap.** Exponentially growing cultures of wild type (*DOA4*) or *tah22* (*doa4-10*) cells, transformed with *ARS/CEN* vectors YCpScTOP1, YCpSctop1T722A, or pRS416, were serially diluted and spotted onto SC-uracil media. Cell viability was assessed following incubation at 26 °C (permissive conditions) or 36 °C (nonpermissive conditions).

additional *TAH* genes, *DOA4*, *SLA1*, and *SLA2*, also protect cells from Top1p poisons.

In backcrosses, the ts phenotype of individual *tah* mutants segregated as a recessive, single gene defect. As the strains were *top1*Δ, cell viability could be assessed in the presence or absence of plasmid-encoded Top1p or Top1T722Ap. Wild type cells were viable at 26 and 36 °C, independent of *TOP1* or *top1T722A* expression (Fig. 1). Furthermore, low levels of vector expressed Top1p were insufficient to confer CPT sensitivity (Tables II and III). In contrast, the viability of *tah22* cells expressing *top1T722A* was diminished at 36 °C, which was further exacerbated by CPT (Fig. 1 and Tables II and III). Similar patterns of conditional sensitivity to *top1T722A* and CPT were observed with *tah6*, *tah14*, and *tah20* cells (Tables II and III; not shown). Consistent with other *tah* mutants, such as *cdc45-10* and *dpb11-10* (7, 39), these mutants exhibited ts hypersensitivity to the DNA replication inhibitor, HU (Table II). However, the lack of *tah22* and *tah14* enhanced sensitivity to DNA-damaging agents, such as the alkylating agent methyl methanesulfonate and UV light (Table II), suggest selective alterations in these mutant strains in response to DNA replication-induced lesions.

As detailed under "Experimental Procedures," *TAH22* was identified as *DOA4, TAH6/TAH20* as *SLA1* and *TAH14* as *SLA2*. Hereafter, *tah22* is *doa4-10*, and *tah14* is *sla2-10*. Further studies focused on *tah6* (*sla1-10*), as the *tah* phenotype was more pronounced than with the *tah20* mutant.

DOA4 encodes a deubiquitinating enzyme (DUB) that associates with the 26 S proteasome to maintain ubiquitin homeostasis by removing poly-ubiquitin chains from proteins targeted for proteasomal degradation (41, 42). Doa4p also functions at a late stage in endocytosis to recycle ubiquitin from plasma membrane proteins targeted for vacuolar degradation (43). One mechanism then, of potentiating the cytotoxic activity of Top1T722Ap or CPT, would be increased Top1p levels either as a direct consequence of defective ubiquitin-mediated proteolysis or as indirect effects on protein turnover. To address this, extracts were prepared of *DOA4* and *doa4-10* cells transformed with YCpScTOP1 or YCpSctop1T722A, grown at 26 °C, and then shifted to 36 °C for 4–24 h. Western blot analysis revealed no variation in Top1p or Top1T722Ap levels (data not shown), whereas the specific catalytic activity of wild type and mutant enzymes in plasmid DNA relaxation assays was unaffected by temperature shift (Fig. 2). As reported previously (26), Top1T722Ap activity was ~5-fold lower than comparable levels of Top1p. However, the extent of TopT722Ap-catalyzed plasmid DNA relaxation was identical in extracts prepared from *doa4-10* and *DOA4* strains grown at 26 or 36 °C (compare lanes highlighted with a *single* and *double asterisk*, respectively, in Fig. 2). As the ts phenotype of *doa4-10* cells was more pronounced on solid media, cells were also harvested from plates, again with no detectable difference in Top1p or Top1T722Ap levels or activity (data not shown). Thus, the enhanced sensitivity of *doa4-10* cells to Top1p poisons was not due to alterations in enzyme stability.

The *doa4-10* mutant contained a nonsense mutation at residue Gln-388. As diagrammed in Fig. 3, truncation of Doa4p eliminates catalytic residues necessary for ubiquitin isopeptidase activity but retains the rhodanese domain. This domain is a structural module in sulfur transferases and the Cdc25 family of phosphatases (57). A subset of dual specificity phosphatases and DUBs also contain a rhodanese domain, including yeast Doa4p, Ubp5p, and human Ubp8p. However, in these instances, the domain lacks the active site Cys and is thought to play a regulatory role or function in substrate recognition.

To determine whether the N-terminal rhodanese domain was expressed in *doa4-10* cells, an HA tag was engineered at the C terminus of Doa4p (Doa4-HAp) or at the position of the nonsense mutation in *doa4-10* (Doa4-10-HAp). The HA tag strains exhibited the same patterns of *top1T722A* and HU sensitivity as the controls. Although Doa4-HAp was readily apparent in immunoblots of cell extracts, Doa4-10-HAp was only sporadically detected in extracts of cells cultured at 36 °C (data not shown). Osmotic stabilizers, salt extraction, and immunoprecipitation failed to resolve this variability. Yet comparisons of *doa4-10* and *doa4*Δ strains revealed considerable phenotypic differences (Table II). *doa4*Δ cells alone exhibited a slow growth phenotype at 36 °C (as reported in Ref. 58) and were hypersensitive to HU at all temperatures. In contrast, only *doa4-10* cell growth was impaired in the presence of high salt. These data suggest that the rhodanese domain induces a distinct set of cellular responses from that observed in *doa4*Δ cells. However, as both strains exhibited a *tah* ts phenotype (Table II), the loss of the DUB catalytic residues sufficed to sensitize yeast to *top1T722A*-induced DNA damage. This appeared to be restricted to Doa4p-regulated events, as deletion of the closely related Ubp5p, or more distinct Ubp11p and Ubp12p, failed to enhance the cytotoxic activity of Top1T722Ap or CPT (data not shown).

SLA1 and *SLA2* were initially identified in a genetic screen for mutants that were synthetically lethal with *abp1*Δ (45). Both gene products function in polarized cell growth and are required for normal cortical cytoskeletal organization. Sla1p is a component of cortical actin patches and plays a role in endocytosis (45, 59). The interaction of Sla1p with Sla2p also affects endocytosis by regulating actin dynamics (46). The *sla1-10* allele (Fig. 3) contained a nonsense mutation at Trp-500 and a Glu-188 to Lys substitution. Comparisons of *sla1-10* and *sla1*Δ strains failed to discern any phenotypic differences (Table II, data not shown), and neither strain was ts for growth at temperatures up to 36 °C. *SLA1* mutations in *tah20* were not defined nor were *SLA2* alterations in *sla2-10*.

Genetic Interactions between DOA4, SLA1, SLA2, and CDC45—To ascertain whether Doa4p was functionally linked to the diverse set of *tah* mutants isolated in our screen, *doa4-10,tah* double mutants were examined. In contrast to the single mutants, double *sla1-10,sla2-10*, *doa4-10,sla1-10*, and *doa4-10,sla2-10* mutants were all inviable at 36 °C in the absence of DNA damage (Fig. 4 and data not shown). A similar synthetic lethal phenotype was observed with *doa4-10* or *doa4*Δ in combination with *sla1*Δ. Genetic and functional interactions between *SLA1* and *SLA2* have been reported (45); however, our results suggest Doa4p also shares an essential function with Sla1p and Sla2p.

The combination of *doa4-10,cdc45-10* induced a ts growth

TABLE II
doa4 and sla1 mutant sensitivity to DNA damage, high salt,and glycerol

Yeast strain[a]	Cell viability at the nonpermissive temperature[b]						
	top1T722A[c]	CPT[c]	HU[d]	MMS[d]	Glycerol[e]	NaCl[d]	UV[f]
Wild type	+++	++++	++++	++++	++++	++++	++++
doa4-10 (*tah22*)	+	+	−	++++	+	+/−	++++
*doa4*Δ	−[g]	ND	−[h]	ND	−	++++	ND
sla1-10 (*tah6*)	+	+	−	+	−	−[h]	++
*sla1*Δ	+	ND	ND	ND	−	−[h]	ND
sla2-10 (*tah14*)	+	+	−	++++	−	++++	++++

[a] Isogenic *top1*Δ yeast strains, wild-type for *DOA4*, *SLA1,* and *SLA2*, or containing the indicated *doa4*, *sla1,* or *sla2* mutant allele were used.
[b] For the conditions indicated, exponentially growing cells, adjusted to an A_{595} = 0.3, were serially 10-fold diluted, and 5-μl aliquots were spotted onto plates. After 3 days at 26 or 36 °C, viability was scored as ++++ for colonies at 10^{-3} dilution, +++ for colonies at 10^{-2}, ++ for colonies at 10^{-1}, + for colonies in undiluted samples, +/− for small colonies in undiluted samples, and − for no growth at 36 °C. ND indicates not determined.
[c] To assay *top1T722A* sensitivity, cells transformed with YCpSctop1T722A were spotted on SC-uracil media and incubated at 26 or 36 °C. YCpScTOP1 was a negative control. For CPT sensitivity, YCpScTOP1 transformants were plated on selective media with 25 mM HEPES, pH 7.2, and 0 or 5 μg/ml CPT in a final 1.25% Me_2SO.
[d] Sensitivity to HU (5 mg/ml), methyl methanesulfonate (MMS) (0.0125%), and 6% NaCl was assayed on YPD plates.
[e] Growth was assessed on yeast extract, peptone, 3% glycerol plates.
[f] UV sensitivity was assessed by colony formation on YPD plates following irradiation with 0, 10, or 20 μJ/M^2 UV and growth at 36 °C.
[g] *doa4*Δ cells exhibited a slow growth phenotype at 36 °C.
[h] Indicates no growth at 26or 36 °C.

TABLE III
*doa4-10, sla1-10, and tdp1*Δ *strains exhibit enhanced sensitivity to Top1T722Ap and CPT*

Yeast strain[a]	*top1* allele[b]	Cell viability[c]			
		26 °C		36 °C	
		No drug	CPT	No drug	CPT
Wild type	*TOP1*	1.0	0.87 ± 0.05	0.93 ± 0.05	0.89 ± 0.04
	top1T722A	1.0	0.9 ± 0.07	0.87 ± 0.05	0.63 ± 0.008
doa4-10	*TOP1*	1.0	0.98 ± 0.11	0.99 ± 0.04	0.83 ± 0.07
	top1T722A	1.0	0.98 ± 0.09	0.075 ± 0.0021	0.0021 ± 0.0014
sla1-10	*TOP1*	1.0	0.97 ± 0.05	1.04 ± 0.07	0.87 ± 0.1
	top1T722A	1.0	0.87 ± 0.16	0.57 ± 0.14	0.0053 ± 0.0028
*tdp1*Δ	*TOP1*	1.0	0.85 ± 0.06	1.03 ± 0.12	0.85 ± 0.02
	top1T722A	1.0	0.86 ± 0.05	0.81 ± 0.14	0.31 ± 0.1
*doa4-10,tdp1*Δ	*TOP1*	1.0	0.93 ± 0.02	0.99 ± 0.13	0.55 ± 0.07
	top1T722A	1.0	0.46 ± 0.16	0.0036 ± 0.00016	<0.00006 ± 0.0000001

[a] As in Table II, isogenic *top1*Δ yeast strains, wild-type for *DOA4, SLA1,* and *TDP1*, or harboring the indicated mutant allele were used.
[b] Cells were transformed with ARS/CEN vectors that constitutively express low levels of *TOP1* or *top1T722A* from the yeast *TOP1* promoter.
[c] Exponentially growing cultures of individual transformants at 26 °C were adjusted to an A_{595} = 0.3 and serially 10-fold diluted, and aliquots were plated on selective media supplemented 5 μg/ml CPT in a final 1.25% Me_2SO or Me_2SO alone (no drug). For each strain and vector, the number of viable cells forming colonies were counted on duplicate sets of plates following incubation at 26 or 36 °C and tabulated relative to the number obtained at 26 °C on the no drug control. Each value is the average of three independent experiments.

defect (Fig. 4). Cdc45p is essential for the initiation of DNA replication (60). We reported previously that the *cdc45-10* mutant, isolated in our *tah* screen, transiently accumulates Okazaki-sized DNA fragments in early S-phase and is required with Dpb11p for processive DNA replication (39). A similar slow growth phenotype at 35 °C was observed with *cdc45-10,rad9*Δ cells (39).

Taken together, these data indicate that the defects in DNA replication induced by *cdc45-10* may be exacerbated by the loss of Doa4p function. As with *rad9*Δ, this may be a consequence of inappropriate DNA damage/S-phase checkpoint responses leading to alterations in cell cycle arrest. Given the genetic interactions between *DOA4*, *SLA1*, and *SLA2*, such events might arise from alterations in cell morphology and actin cytoskeleton reorganization as cells progress through the cell cycle. To address these issues, *doa4-10* and *sla1-10* cell morphology was examined.

doa4-10 and sla1-10 Mutants Exhibit Alterations in Cell Morphology—Wild type and mutant strains, grown at 26 °C or shifted to 36 °C, were fixed and stained with rhodamine-phalloidin to visualize the distribution of F-actin. In representative images of wild type *DOA4* cells (Fig. 5, *a–h*), cortical actin patches concentrate at the incipient bud site (*a* and *b*). As the bud emerges (*c* and *d*), cortical actin patches are mostly confined to the apical end of the bud (*single arrow*), with actin cables aligned with the axis of bud growth (*double arrows* in *e* and *f*). A switch

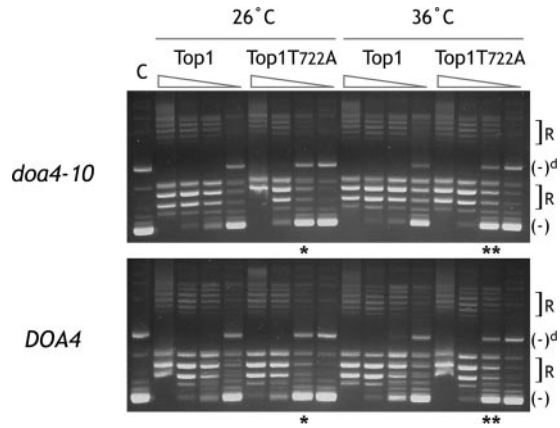

FIG. 2. **Top1T722Ap-specific catalytic activity is unaltered in *doa4-10* cells.** Extracts of *doa4-10* or *DOA4* cells transformed with YCpScTOP1 or YCpSctop1T722A were prepared from exponential cultures grown at 26 °C or shifted to 36 °C for 6 h. After correcting for total protein concentration, the extracts were 10-fold serially diluted and incubated in plasmid DNA relaxation reactions as described under "Experimental Procedures." The reaction products were resolved in an agarose gel and visualized by ethidium bromide staining. The positions of negatively supercoiled DNA monomers (−) and dimers $(-)^d$, and relaxed topoisomers (*R*) are indicated. *Lane C* is untreated plasmid DNA. Samples incubated with a 10^{-2} dilution of extracts prepared from strains expressing *top1T722A* at 26 or 36 °C are indicated by * or **, respectively.

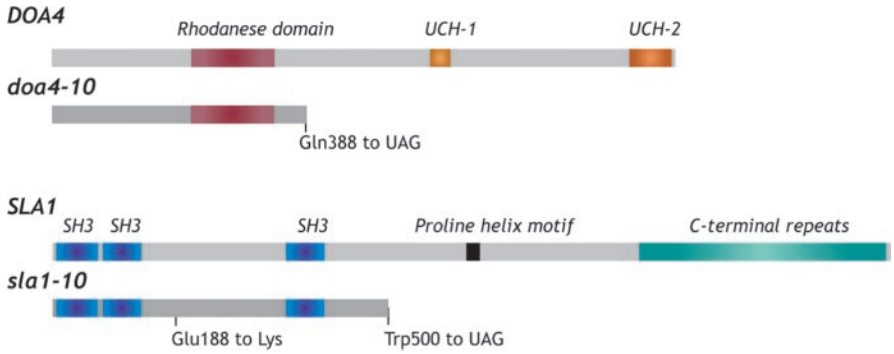

FIG. 3. ***doa4-10* and *sla1-10* alleles contain nonsense mutations.** *Top*, in *doa4-10*, the codon encoding glutamine 388 has been mutated to a nonsense codon. The stop codon eliminates the hydrolase active site (UCH-1 and UCH-2 in *orange*) but retains a rhodanese domain (in *red*) implicated in protein-protein interactions. *Bottom,* in *sla1-10*, a single nucleotide substitution changed Trp-500 to a translational stop, and a second mutation substitutes Lys for Glu-188.

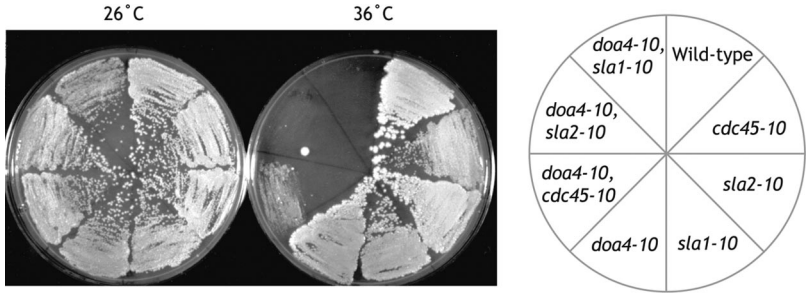

FIG. 4. ***doa4-10* exhibits a synthetic lethal interaction with *sla1-10* or *sla2-10* and a slow growth phenotype in combination with *cdc45-10*.** Single mutant strains *doa4-10* (RRY92), *sla1-10* (RRY76), *sla2-10* (RRY84), and *cdc45-10* (RRY72) and the double mutants *doa4-10,sla1-10* (MSY61), *doa4-10,sla2-10* (MSY75), and *doa4-10,cdc45-10* (MSY6), streaked on YPD plates, were incubated at 26 and 36 °C.

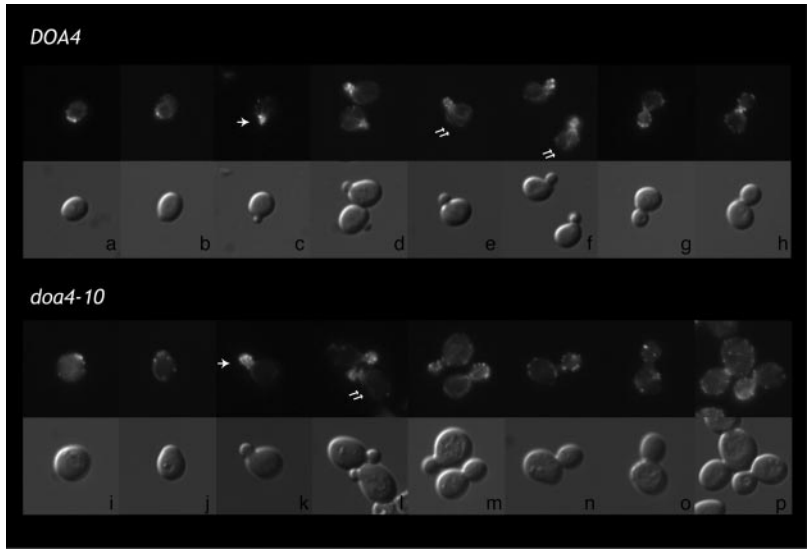

FIG. 5. ***doa4-10* cells exhibit alterations in actin staining.** Wild type *DOA4* (EKY3) and *doa4-10* (RRY92) cells, grown at 36 °C in YPD media, were fixed with formaldehyde and stained with rhodamine-phalloidin to visualize F-actin as described under "Experimental Procedures." Paired DIC and phalloidin-stained images are arranged in order of increasing bud size for DOA4 cells (*a–h*) and *doa4-10* cells (*i–p*). *Single arrows* indicate cortical actin patches localized in the bud, and *double arrows* highlight actin cables radiating into the mother cell.

to isotropic bud growth is accompanied by a redistribution of actin patches over the bud surface (*g*), and following cytokinesis, the patches relocalize to the mother-bud junction (*h*).

As reported previously (45) for *sla1*Δ strains, *sla1-10* cells exhibit gross defects in cortical actin patch organization, with a few large patches visible per cell (data not shown). The alterations in *doa4-10* cell morphology were more subtle. First, *doa4-10* cells cultured at 36 °C were larger in size, particularly the large-budded cells, with evidence of autophagic bodies and cell lysis in the DIC images (data not shown). A survey of >400 DAPI-stained cells indicated ~45% of *doa4-10* cells were large-budded, ~60% of which had a single nuclear mass. Corresponding values for *DOA4* cells cultured under the same conditions were ~27 and 30%, respectively. Moreover, in contrast to wild type cells, a significant percentage of *doa4-10* and *sla1-10* cells were lysed (6 and 10%, respectively). Most of the ghosts appeared to have large buds. Double *doa4-10,sla1-10* mutants were particularly fragile, with extensive cell lysis and clumping evident shortly after shift to 36 °C.

The pattern of actin staining in *doa4-10* cells was consistent with these alterations in cell cycle distribution (Fig. 5, *i–p*). The cortical patches were appropriately localized to the bud site and emerging bud (*i–l*). Actin cables radiating into the mother cell were apparent (*double arrows, l*), although not as well organized as in wild type *DOA4* cells. As bud size increased (*n–p*), the actin patches became isotropically distributed and the cables more diffuse. In many large-budded cells with segregated nuclear masses, the actin patches failed to relocalize to the mother-bud junction (compare *n* and *p* with *h*), consistent with a defect in cytokinesis in *doa4-10* cells. Whether this is caused by actin cytoskeletal defects or is simply reflected by the isotropic distribution of actin patches and cables has yet to be addressed.

Electron microscopy was also used to examine *doa4* and *sla1* mutant cell morphology. In contrast to wild type cells (Fig. 6*A*), enlarged and fragmented vacuoles are evident in ~30% of the *doa4-10* cells grown at 36 °C. As reported for *sla1*Δ cells (44, 46, 59), thick cell walls were also evident in *sla1-10* mother cells but not in the bud. Significant cell lysis was apparent, with discontinuities in cell wall structure visible at the mother-bud juncture (Fig. 6*A*). Lysis was more pronounced with the double *doa4-10,sla-10* mutant, coincident with more severe cell wall

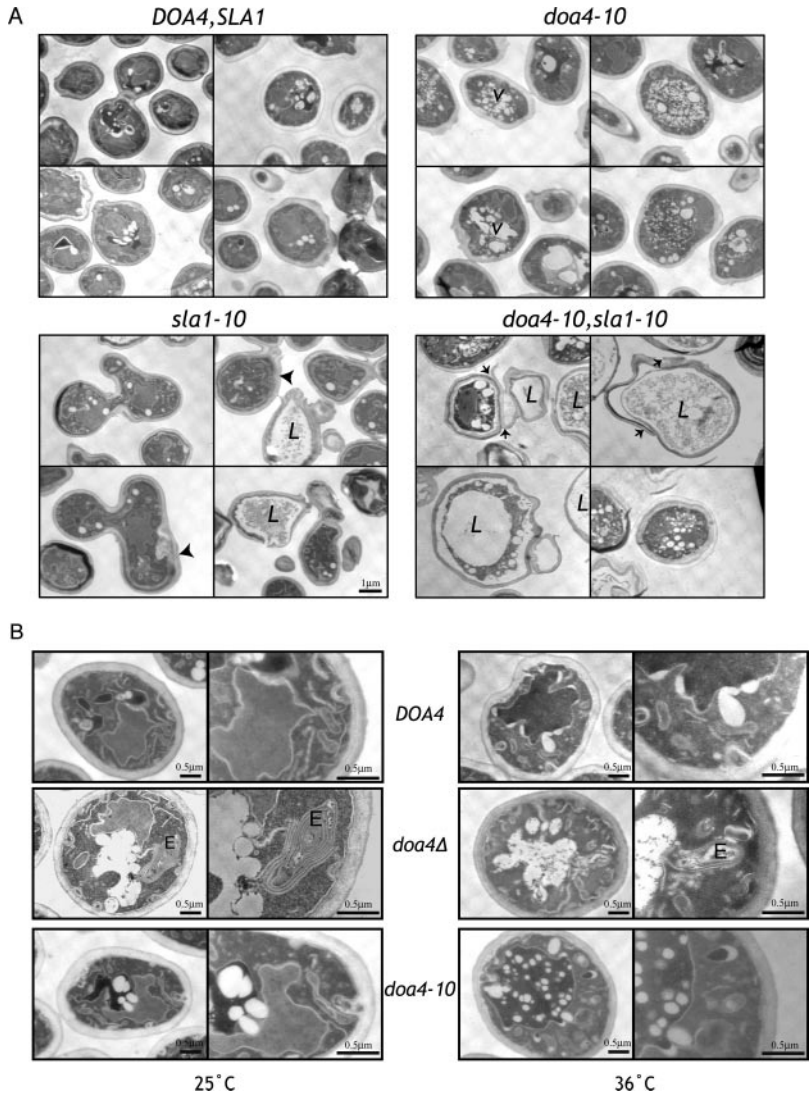

FIG. 6. **Morphology of *doa4* and *sla1* mutants.** Cultures of wild type *DOA4* (EKY3), *doa4-10* (RRY92), *doa4*Δ (MSY85), *sla1-10* (RRY76), and *doa4-10,sla1-10* (MSY61) cells, shifted to 36 °C for 10 h, were fixed, embedded, and visualized by electron microscopy as described under "Experimental Procedures." *A*, *V* indicates enlarged vacuoles in *doa4-10* cells and *L* indicates *sla1-10* or *doa4-10, sla-10* ghosts. *Arrowheads* indicate the thick cell walls of *sla1-10* cells, and the *small arrows* point to the multiple cell wall layers of *doa4-10,sla1-10* cells. *B*, *E* indicates the stacked cisternal membranes of the class E compartments detected at 26 and 36 °C in *doa4*Δ but not *doa4-10* cells. The images on the *right* are higher magnification views of the cells pictured on the *left*.

defects. At 26 °C, double or triple cell wall layers were evident in ~40% of the double mutant cells. At 36 °C, 80% of the cells had multiple cell wall layers; 40% of the cells were lysed ghosts, and 30% of these were 2–3 times larger than wild type cells. As seen in Fig. 6*A* (*doa4-10,sla1-10*), some layers appeared to have pealed away from the cell wall structure. Whether this induces, or results from, cell lysis remains unclear.

Comparisons of *DOA4* cells with *doa4*Δ and *doa4-10* mutants further distinguished *doa4*Δ cells from cells expressing the N-terminal rhodanese domain of Doa4p. In addition to alterations in vacuolar architecture, 25-30% of *doa4*Δ cells accumulated stacks of curved cisternal membranes, independent of temperature (Fig. 6*B*). These structures resemble pre-vacuolar class E compartments reported in some *vps* mutants (52). Doa4p functions late in endocytosis to remove ubiquitin from plasma membrane proteins targeted for vacuolar degradation; however, class E endosomal compartments have not been reported in *doa4* mutants (43). In contrast, stacked membranes were not detected in *doa4-10* cells at either temperature, suggesting that the loss of Doa4p catalytic activity is insufficient to elicit this phenotype.

Given the role of Doa4p in endocytosis and vacuolar mediated degradation, the possibility remained that defects in endocytosis, and not ubiquitin homeostasis *per se*, enhanced *doa4-10* cell sensitivity to Top1p poisons. However, deletion of *VPS4*, which functions immediately after Doa4p in the formation of vesicles that fuse with the vacuole (61), had no effect on cell sensitivity to *top1T722A* or CPT (data not shown). Instead, *vps4*Δ complemented the *tah* phenotype of *doa4-10* cells, supporting the notion that other DUBs recycle ubiquitin from plasma membrane proteins that accumulate in the pre-vacuolar compartment. Thus, defects in endocytosis and vacuolar mediated degradation did not modulate cell sensitivity to Top1p-induced DNA lesions.

Dosage Suppressors of doa4-10 top1T722Ap-Hypersensitivity—To address more directly the mechanism of Doa4p protection against Top1p poisons, dosage suppressors of *top1T722A*-induced *doa4-10* cell death at 36 °C were isolated from a YEp-FY250 genomic DNA library (detailed under "Experimental Procedures"). Consistent with the *vps4*Δ,*doa4-10* results, increased dosage of the ubiquitin genes *UBI4* and *UBI2* suppressed *doa4-10* hypersensitivity to *top1T722A* and HU at 36 °C (data not shown, Fig. 7*A*). YEpUBI2 and YEpUBI4 also rescued *doa4-10* temperature sensitivity to high salt and glycerol (data not shown).

In contrast, *SML1* was a selective, albeit weak, dosage suppressor of *doa4-10* hypersensitivity to *top1T722A* at 36 °C (Fig. 7*B*). Sml1p inhibits ribonucleotide reductase, an enzyme induced by Mec1p/Rad53p kinases following induction of the S-phase checkpoint (47, 62). Deletion of *SML1* restores *mec1*Δ or *rad53*Δ cell viability but not checkpoint function. The Mec1p/Rad53p kinase cascade also targets Sml1p for degradation following checkpoint activation (63). *sml1*Δ cells were not hypersensitive to *top1T722A* or CPT (Table IV, data not shown);

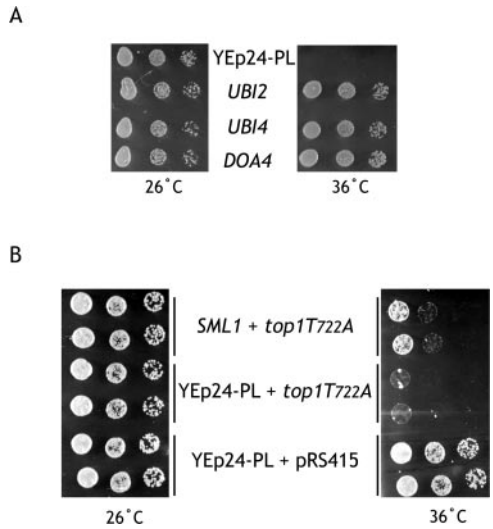

FIG. 7. ***UBI2, UBI4,* and *SML1* are dosage suppressors of *doa4-10.*** *A*, *doa4-10* (RRY92) cells transformed with YEpUBI2, YEpUBI4, YEpDOA4, or vector alone (YEp24-PL) were serially diluted, and 5-μl volumes were spotted onto SC-uracil plates supplemented with 10 mg/ml HU. *B*, *doa4-10* (RRY92) cells were co-transformed with YCpSctop1T722A-L (or pRS415 vector control) and YEpSML1 (or YEp24-PL vector control), serially diluted, and spotted onto SC-uracil, -leucine media. Cell viability was assessed following incubation at 26 and 36 °C.

thus, the activity of *SML1* as a dosage suppressor could not be attributed to a direct effect on Sml1p stability or turnover. An alternative possibility is that increased Sml1p levels reinforce activation of the Mec1p-Rad53p checkpoint, thereby slowing S-phase progression and/or enhancing replication fork stability and diminishing Top1p poison-induced DNA lesions. This model requires a functional *MEC1/RAD53* checkpoint in *doa4-10* cells and may derive from the inactivation of other DNA damage checkpoint functions. Indeed, the latter point would be consistent with the ts slow growth phenotype of the *cdc45-10* mutant in combination with either *doa4-10* (Fig. 4) or *rad9*Δ (39) and the accumulation of *doa4-10* cells with a large-budded phenotype in the absence of DNA damage.

DNA Damage and S-phase Checkpoints Protect against Top1p Poisons—As shown in Fig. 8, *doa4-10* cells respond to HU-induced activation of the S-phase checkpoint. Wild type and mutant strains, cultured at 26 °C, were left untreated or treated with HU prior to shift to 36 °C. In the presence of HU, over 85% of wild type and *doa4-10* cells arrested as large-budded cells, over 90% of which had a single nuclear mass (data not shown). HU-treated *sla1-10* and *doa4-10, sla1-10* cells also arrested with a similar phenotype, although at later times, *sla1-10* viability decreased due to cell lysis (Fig. 8, data not shown). This effect was exacerbated with the double *doa4-10,sla1-10* mutant, consistent with the structural fragility of large-budded cells indicated in Fig. 6*A*. These findings suggest that the cell wall defects induced by *sla1-10*, which enhance large-budded cell fragility at high temperature, underlie the enhanced sensitivity of *sla1* mutants to Top1T722Ap-induced lesions during S-phase. However, these data also demonstrate a functional *MEC1/RAD53* checkpoint in *doa4-10* and *sla1-10* strains.

To examine potential interactions between Doa4p and S-phase checkpoint components (reviewed in Refs. 64 and 65), *DOA4* and *doa4-10* strains were deleted for *RAD9, TOF1, RAD24, RAD17, MEC1, RAD53, CHK1*, or *TEL1* and assayed for enhanced sensitivity to *top1T722A* or CPT. The results are summarized in Table IV. We reported that Rad9p protects cells from low levels of Top1p poisons (39). Consistent with earlier reports of CPT sensitivity (26, 28–34, 66), strains deleted for *RAD17*, *RAD24*, *MEC1* (*sml1*Δ), and *RAD53* (*sml1*Δ) were hypersensitive to *top1T722A*. However, the *rad9*Δ, *rad17*Δ, and *rad24*Δ data obtained here indicate Top1T722Ap-induced damage was more cytotoxic than lesions induced by CPT. Tel1p and Tof1p also protected against Top1p poisons. In contrast to *Schizosaccharomyces pombe* (67), *chk1*Δ cells were no more sensitive to Top1T722Ap or CPT than wild type cells. Although Chk1p may function in response to higher concentrations of CPT, these data preclude a significant role for Chk1p at low levels of Top1p poisons.

In combination with *doa4-10*, all checkpoint mutants were either more sensitive to Top1p poisons or as sensitive as the single checkpoint null strain (Table IV). The exception was the *doa4-10,rad9*Δ double mutant, where the cold sensitivity of *rad9*Δ cells to *top1T722A* and CPT was partially suppressed by the *doa4-10* mutation. Similarities in *doa4-10* and *doa4-10,rad9*Δ sensitivity to *top1T722A* and CPT suggest *doa4-10* is epistatic to *rad9*Δ, although in a manner distinct from Rad24p/Rad17p, Chk1p, or Mec1p/Rad53p.

Doa4 and Tdp1 Act in the Distinct Pathways in Response to Top1p-DNA Damage—To extend these findings, tyrosyl DNA phosphodiesterase I (Tdp1p) function was also examined. Tdp1p specifically hydrolyzes the 3′-phosphotyrosyl linkage between Top1p and DNA to yield a 3′-phosphoryl DNA end (68). Increasing evidence suggests this enzyme plays an important role in the repair of lesions induced by Top1p-DNA intermediates (37, 38). Pouliet *et al.* (68) demonstrated the enhanced sensitivity of *tdp1*Δ cells to Top1p poisons when the *RAD9* gene was deleted, positing that Rad9p and Tdp1p constitute parallel pathways that protect cells from CPT. Consistent with this view, the enhanced sensitivity of *doa4-10* cells to low constitutive levels of Top1T722Ap or CPT-induced DNA damage at 36 °C is exacerbated in *doa4-10,tdp1*Δ double mutants (Fig. 9 and Table III). Moreover, the double mutant is unable to tolerate Top1T722Ap at any temperature. In contrast, *tdp1*Δ cells were CPT-resistant at all temperatures and only exhibit enhanced sensitivity to Top1T722Ap at 36 °C when co-treated with CPT. Thus, defects in Doa4p function potentiate the cytotoxic activity of low doses of Top1p poisons in cells deleted for *TDP1*.

DISCUSSION

To investigate cellular processes that protect cells from the cytotoxic activity of chemotherapeutics that target DNA topoisomerase I, a yeast genetic screen was developed to isolate conditional mutants exhibiting enhanced sensitivity to low levels of a self-poisoning Top1T722A mutant enzyme (39). Here we report that mutations in the non-essential genes *DOA4*, *SLA1*, and *SLA2* potentiate the cytotoxic activity of the Top1p poison CPT and Top1T722Ap. Furthermore, consistent with the S-phase specificity of drugs that target DNA topoisomerase I, these *tah* mutants were also hypersensitive to HU at the non-permissive temperature (Table II). These data indicate that alterations in ubiquitin homeostasis, due to the loss of Doa4p catalytic residues, or actin cytoskeletal organization, resulting from the loss of Sla1p or Sla2p function, abrogate the ability of the cell to tolerate low levels of Top1p poison-induced DNA lesions.

Although detection of the truncated Doa4-10-HA protein proved difficult, phenotypic differences between *doa4*Δ and *doa4-10* cells provided indirect evidence of rhodanese domain function. Perhaps most compelling was the selective accumulation of pre-vacuolar E class vesicles evident in *doa4*Δ cells but absent in congenic *doa4-10* strains (Fig. 6*B*). Differences in growth rate at 36 °C, temperature-sensitive growth in the presence of high salt, and the enhanced sensitivity of *doa4*Δ to HU

TABLE IV
DNA damage checkpoint defective yeast strains are hypersensitive to Top1p poisons

Yeast strain[a]	Cell viability[b]					
	26 °C			36 °C		
	CPT	top1T722A	Vector	CPT	*top1T722A*	Vector
Wild type	++++	++++	++++	++++	+++	++++
doa4-10	+++	+++	++++	+	−	++++
rad17Δ	+	−[c]	++++	+++	−[c]	++++
doa4-10,rad17Δ	−	−[c]	++++	−	−[c]	++++
rad24Δ	+	−[c]	++++	+++	−[c]	++++
doa4-10,rad24Δ	+	−[c]	++++	−	−[c]	++++
rad9Δ	+	+	++++	+++	+	++++
doa4-10,rad9Δ	++	++	++++	+	+	++++
tel1Δ	+++	+++	++++	+	−	++++
doa4-10,tel1Δ	+	++	++++	−	−	++++
tof1Δ	−	+	++++	+++	+	++++
doa4-10,tof1Δ	−	+	++++	−	+	++++
chk1Δ	++++	+++	++++	++++	+++	++++
doa4-10,chk1Δ	+++	+++	++++	+	−	++++
doa4-10,sml1Δ	+++	+++	++++	+	−	++++
sml1Δ,rad53Δ	−	−[c]	++++	−	−[c]	++++
doa4-10,sml1Δ,rad53Δ	−	−[c]	++++	−	−[c]	++
sml1Δ,mec1Δ	−	−[c]	++++	−	−[c]	++++
doa4-10,sml1Δ,mec1Δ	−	−[c]	+++	−	−[c]	+++

[a] See Table I for genotypes.
[b] The indicated yeast strains, transformed with YCpSctop1T722A (*top1T722A*), YCpScTOP1 (CPT), or pRS416 (vector) were assayed for cell viability at 26 and 36 °C in the presence or absence of CPT, as described in the legend to Table II.
[c] No transformants were obtained.

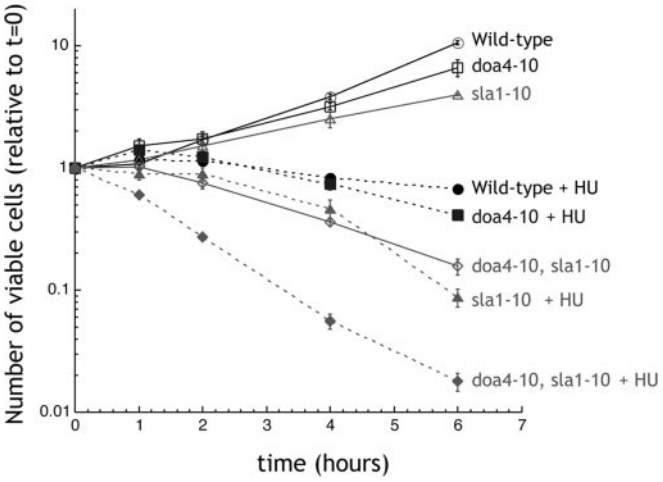

FIG. 8. **HU treatment exacerbates the synthetic lethal phenotype of *doa4-10,sla1-10* cells.** Exponentially growing cultures of wild type (EKY3), *doa4-10* (RRY92), *sla1-10* (RRY76). and *doa4-10,sla1-10* (MSY61) cells at 26 °C were split in two; one-half was treated for 30 min with 15 mg/ml HU, and then both cultures were shifted to 36 °C. At the times indicated, aliquots were withdrawn and serially diluted, and the number of viable cells forming colonies was determined by plating on YPD media at 26 °C. For each treatment, the number of cells was plotted relative to that obtained at $t = 0$. Values are the average of at least three experiments, and standard errors are included.

at all temperatures were also suggestive of rhodanese domain function (Table II). However, the DUB activity of Doa4p appeared critical for cellular resistance to Top1p poisons, as both *doa4-10* and *doa4Δ* strains exhibited enhanced sensitivity to Top1T722Ap and CPT.

Deletion of *VPS4* inhibits a late step in endocytosis, immediately downstream of Doa4p-catalyzed recycling of ubiquitin from membrane proteins in multivesicular bodies that are targeted for degradation following vesicle fusion with the vacuole (reviewed in Ref. 69). The ability of *vps4Δ* to complement the *tah* phenotype of *doa4-10*, yet eliminate a critical step in vacuolar trafficking, suggests defects in endocytosis *per se* do not alter cell sensitivity to Top1 poisons. Rather the ability of other DUB activities to recycle ubiquitin from membrane proteins targeted for vacuolar degradation and the isolation of *UBI2* and *UBI4* as dosage suppressors of *doa4-10* argue for a direct effect of ubiquitin homeostasis on cellular responses to these S-phase toxins. Yet this phenotype appears restricted to Doa4p-catalyzed events, as deletion of the closely related Ubc5p or the more distantly related Ubp12 or Ubp11 enzymes had no adverse effects on cell sensitivity to Top1p poisons.

In mammalian cells, transcription-dependent degradation of ubiquitinated Top1p by the 26 S proteasome has been reported in response to high concentrations of CPT (70, 71). Whereas this may constitute a mechanism of CPT resistance, the converse does not appear to be true, *i.e.* the absence of ubiquitin-mediated down-regulation of Top1p enhancing drug sensitivity. The lack of detectable alterations in Top1p or Top1T722Ap protein levels or catalytic activity in extracts of *DOA4* and *doa4-10* cells cultured under a variety of experimental conditions precludes a direct effect of ubiquitin-mediated effects on Top1 protein stability or activity. Indeed, our previous studies of p*GAL1*-promoted expression of *top1T722A* indicate substantially elevated levels of protein expression are required to induce cell lethality in wild type cells (26). The results reported here are inconsistent with the up-regulation of Top1p levels or activity in *doa4-10* mutant cells. Furthermore, alterations in HU sensitivity were Top1p-independent. Whether putative human orthologs of *DOA4*, such as *UBP8* or *UBP2*, play a similar role in modulating human cell sensitivity to Top1p poisons is currently being investigated with small interfering RNA approaches.

Genetic interactions between *SLA1* and *SLA2* have been reported (45, 46). However, the ts synthetic lethality of *doa4* mutants in combination with *sla1* or *sla2* mutants in the absence of DNA damage was surprising. Morphological inspection of the single and double mutants indicated that the defects in cell wall structure, reported for *sla1* mutants (44, 46, 59), was exacerbated by the loss of Doa4p DUB activity. The result was a pronounced increase in cell lysis, particularly at the large-budded stage of the cell cycle. The obvious prediction that accumulation of cells with large buds would enhance cell fragility was also borne out by the dramatic drop in *doa4-10,sla1-10* double mutant cell viability in response to HU activation of the S-phase checkpoint. Cell fragility could be a consequence of defects in cell wall structure due to Doa4p-

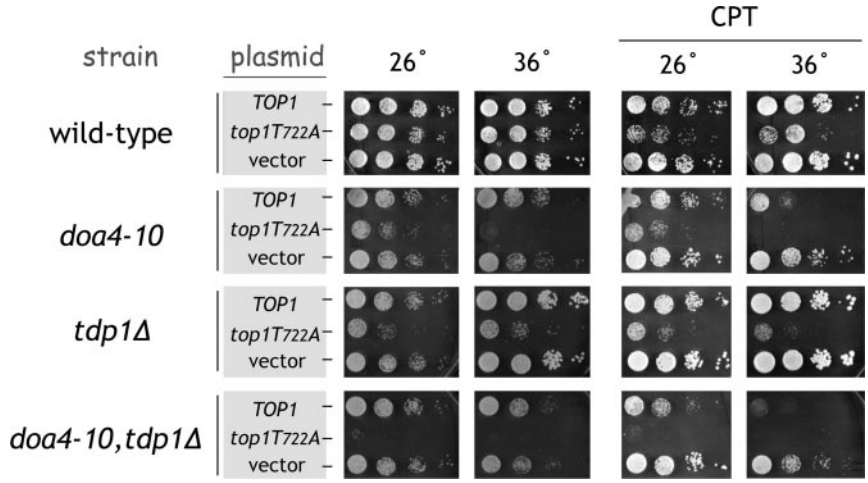

FIG. 9. **Doa4p and Tdp1p act in distinct pathways to protect cells from TopT722Ap-induced DNA damage.** Exponentially growing cultures of wild type (EKY3), *doa4-10* (RRY92), *tdp1*Δ (PFY68), and *doa4-10,tdp1*Δ (PFY67) cells transformed with *ARS/CEN* vectors constitutively expressing the indicated *TOP1* allele or vector control were serially diluted and spotted onto selective media alone (*left panels*) or plates supplemented with 25 mM HEPES, pH 7.2, 1.25% Me_2SO, and 5 μg/ml CPT (*right panels*). Cell viability was assessed after incubation at 26 or 36 °C.

mediated effects on vesicle trafficking. However, in a recent proteomics approach to identify ubiquitinated proteins in yeast, Sla1p and Sla2p were among the proteins identified (72). This raises the interesting possibility that ubiquitin conjugation may directly affect Sla1p and Sla2p function. Whether cell lysis is restricted to the late S/G_2 cell cycle compartment or would also be evident in response to mitotic poisons, such as nocodazole, has yet to be determined. Nevertheless, our results establish a functional link between ubiquitin homeostasis, actin cytoskeletal organization, and cellular resistance to Top1p poisons.

Insights into potential mechanisms of Doa4p-mediated protection from Top1p-induced DNA damage came from the isolation of *SML1* as a selective albeit weak dosage suppressor of *doa4-10* temperature sensitivity to Top1T722A. Sml1p inhibition of ribonucleotide reductase is antagonistic to the induction of this enzyme by the Mec1p/Rad53p/Dun1p signaling pathway in response to replicative stress (47, 62). Indeed, Zhao *et al.* (63) demonstrated that Sml1p is also targeted for ubiquitin-mediated degradation following activation of the Mec1p/Rad53p checkpoint. As *sml1*Δ cells were not hypersensitive to CPT or Top1T722Ap, it is unlikely that Sml1p down-regulation is the basis for the *doa4-10 tah* phenotype. Furthermore, treatment with HU suffices to induce *doa4-10* cell cycle arrest, providing evidence that at least some aspects of Mec1p/Rad53p signaling pathways remain functional. Taken together, this raises the possibility that increased dosage of Sml1p reinforces activation of the Mec1p/Rad53p signaling pathway, enhancing the DNA damage response and possibly repair.

A survey of replication and DNA damage checkpoint mutants provided further support of genetic interactions between *RAD9* and *DOA4*, as *doa4-10* partially suppressed the enhanced sensitivity of *rad9*Δ cells to *top1T722A* at 26 °C. In contrast, all other *doa4-10* checkpoint mutant combinations examined potentiated the cytotoxic action of Top1p poisons. Several lines of evidence indicate the functional interaction of Doa4p and some aspect of DNA damage signaling. First is the accumulation of large-budded *doa4-10* cells with a single DNA mass at 36 °C, even in the absence of DNA damage. Singer *et al.* (73) reported previously a role for Doa4p in regulating the coordination of DNA replication. However, in their studies, the re-replication of DNA was only observed at 38 °C and was not suppressed by increased levels of *UBI4*. As the *tah* phenotype of *doa4-10* cells was evident at 36 °C and was fully suppressed by increased dosage of *UBI2* or *UBI4*, such a re-replication mechanism seems unlikely. An alternative explanation may be a defect in replication fork stability, which induces DNA repair pathways. Indeed, several recent studies (65, 74, 75) demonstrate Mrc1p and Tof1p function to stabilize stalled replication forks and may prevent the processing of blocked forks to form alternative structures that trigger components of the DNA damage checkpoint, such as Rad9p. Analogous to Rad9p in response to DNA damage, Mrc1p acts as a mediator to activate Rad53p in response to replication stress. Thus, independent mechanisms may enhance signaling through a common kinase cascade. Increased dosage of *SML1* may reinforce the Mrc1p/Tof1p pathway and diminish signaling/repair by Rad9p.

The synthetic slow growth phenotype induced in *rad9*Δ*,cdc45-10* cells upon shift to 35 °C (39) suggests that alterations in processive DNA replication induced by *cdc45-10* trigger the Rad9p-dependent DNA damage checkpoint. The fact that *doa4-10,cdc45-10* cells exhibit a similar phenotype is consistent with the genetic interaction of *DOA4* and *RAD9* in altering cellular responses to Top1T722Ap (Table IV). The enhanced CPT/*top1T722A* sensitivity of *doa4-10* cells deleted for tyrosyl phosphodiesterase I (Table III) also suggests *doa4-10*-induced alterations in repair pathways that act in parallel with Tdp1p to effect the repair of Top1-DNA lesions, such as the Rad9p DNA damage checkpoint (68). Whether this is due to specific alterations in Rad9p function or indirect effects on checkpoint-induced repair activities has yet to be investigated. More thorough analyses of checkpoint signaling and extragenic suppressors of *doa4-10* sensitivity to Top1T722Ap are also being pursued to elucidate the functional link between alterations in Doa4p-mediated ubiquitin homeostasis and cellular response to Top1p poisons.

Acknowledgments—We thank members of the Bjornsti lab for helpful discussions and Alice Gibson, Weiguo Ye, and Mizuno Sugawara for their expert technical assistance.

REFERENCES

1. Wang, J. C. (2002) *Nat. Rev. Mol. Cell. Biol.* **3,** 430–440
2. Champoux, J. J. (2001) *Annu. Rev. Biochem.* **70,** 369–413
3. Pizzolato, J. F., and Saltz, L. B. (2003) *Lancet* **361,** 2235–2242
4. Li, T. K., and Liu, L. F. (2001) *Annu. Rev. Pharmacol. Toxicol.* **41,** 53–77
5. Kohn, K., and Pommier, Y. (2000) *Ann. N. Y. Acad. Sci.* **922,** 11–26
6. Reid, R. J. D., Benedetti, P., and Bjornsti, M.-A. (1998) *Biochim. Biophys. Acta* **1400,** 289–300
7. Fiorani, P., and Bjornsti, M. A. (2000) *Ann. N. Y. Acad. Sci.* **922,** 65–75
8. Cheng, C., Kussie, P., Pavletich, N., and Shuman, S. (1998) *Cell* **92,** 841–850
9. Lesher, D. T., Pommier, Y., Stewart, L., and Redinbo, M. R. (2002) *Proc. Natl. Acad. Sci. U. S. A.* **99,** 12102–12107
10. Redinbo, M. R., Stewart, L., Kuhn, P., Champoux, J. J., and Hol, W. G. J. (1998) *Science* **279,** 1504–1513
11. Stewart, L., Redinbo, M. R., Qiu, X., Hol, W. G. J., and Champoux, J. J. (1998) *Science* **279,** 1534–1541
12. Staker, B. L., Hjerrild, K., Feese, M. D., Behnke, C. A., Burgin, A. B., Jr., and Stewart, L. (2002) *Proc. Natl. Acad. Sci. U. S. A.* **99,** 15387–15392
13. Wang, L.-F., Ting, C.-Y., Lo, C.-K., Su, J.-S., Mickley, L. A., Fojo, A. T., Whang-Peng, J., and Hwang, J. (1997) *Cancer Res.* **57,** 1516–1522
14. Woo, M. H., Vance, J. R., Marcos, A. R., Bailly, C., and Bjornsti, M. A. (2002) *J. Biol. Chem.* **277,** 3813–3822

15. Urasaki, Y., Laco, G. S., Pourquier, P., Takebayashi, Y., Kohlhagen, G., Gioffre, C., Zhang, H., Chatterjee, D., Pantazis, P., and Pommier, Y. (2001) *Cancer Res.* **61,** 1964–1969
16. Tanizawa, A., Bertrand, R., Kohlhagen, G., Tabuchi, A., Jenkins, J., and Pommier, Y. (1993) *J. Biol. Chem.* **268,** 25463–25468
17. Rubin, E., Pantazis, P., Bharti, A., Toppmeyer, D., Giovanella, B., and Kufe, D. (1994) *J. Biol. Chem.* **269,** 2433–2439
18. Li, X. G., Haluska, P., Hsiang, Y. H., Bharti, A. K., Liu, L. F., and Rubin, E. H. (1997) *Biochem. Pharmacol.* **53,** 1019–1027
19. Kubota, N., Kanazawa, F., Nishio, K., Takeda, Y., Ohmori, T., Fujiwara, T., Terashiman, Y., and Saijo, N. (1992) *Biochem. Biophys. Res. Commun.* **188,** 571–577
20. Knab, A. M., Fertala, J., and Bjornsti, M.-A. (1995) *J. Biol. Chem.* **270,** 6141–6148
21. Hann, C. L., Carlberg, A. L., and Bjornsti, M.-A. (1998) *J. Biol. Chem.* **273,** 31519–31527
22. Fujimori, A., Harker, W. G., Kohlhagen, G., Hoki, Y., and Pommier, Y. (1995) *Cancer Res.* **55,** 1339–1346
23. Fiorani, P., Bruselles, A., Falconi, M., Chillemi, G., Desideri, A., and Benedetti, P. (2003) *J. Biol. Chem.* **278**, 43268–43275
24. Fiorani, P., Amatruda, J. F., Silvestri, A., Butler, R. H., Bjornsti, M. A., and Benedetti, P. (1999) *Mol. Pharmacol.* **56,** 1105–1115
25. Benedetti, P., Fiorani, P., Capuani, L., and Wang, J. C. (1993) *Cancer Res.* **53,** 4343–4348
26. Megonigal, M. D., Fertala, J., and Bjornsti, M.-A. (1997) *J. Biol. Chem.* **272,** 12801–12808
27. Fertala, J., Vance, J. R., Pourquier, P., Pommier, Y., and Bjornsti, M.-A. (2000) *J. Biol. Chem.* **275,** 15246–15253
28. Zhang, H., and Siede, W. (2003) *Mutat. Res.* **527,** 37–48
29. Simon, J. A., Szankasi, P., Nguyen, D. K., Ludlow, C., Dunstan, H. M., Roberts, C. J., Jensen, E. L., Hartwell, L. H., and Friend, S. H. (2000) *Cancer Res.* **60,** 328–333
30. Bennett, C. B., Lewis, L. K., Karthikeyan, G., Lobachev, K. S., Jin, Y. H., Sterling, J. F., Snipe, J. R., and Resnick, M. A. (2001) *Nat. Genet.* **29,** 426–434
31. Cliby, W. A., Lewis, K. A., Lilly, K. K., and Kaufmann, S. H. (2002) *J. Biol. Chem.* **277,** 1599–1606
32. Furuta, T., Takemura, H., Liao, Z. Y., Aune, G. J., Redon, C., Sedelnikova, O. A., Pilch, D. R., Rogakou, E. P., Celeste, A., Chen, H. T., Nussenzweig, A., Aladjem, M. I., Bonner, W. M., and Pommier, Y. (2003) *J. Biol. Chem.* **278,** 20303–20312
33. Xiao, Z., Chen, Z., Gunasekera, A. H., Sowin, T. J., Rosenberg, S. H., Fesik, S., and Zhang, H. (2003) *J. Biol. Chem.* **278,** 21767–21773
34. Wang, J. L., Wang, X., Wang, H., Iliakis, G., and Wang, Y. (2002) *Cell Cycle* **1,** 267–272
35. Nitiss, J., and Wang, J. C. (1988) *Proc. Natl. Acad. Sci. U. S. A.* **85,** 7501–7505
36. Bastin-Shanower, S. A., Fricke, W. M., Mullen, J. R., and Brill, S. J. (2003) *Mol. Cell. Biol.* **23,** 3487–3496
37. Liu, C., Pouliot, J. J., and Nash, H. A. (2002) *Proc. Natl. Acad. Sci. U. S. A.* **99,** 14970–14975
38. Vance, J. R., and Wilson, T. E. (2002) *Proc. Natl. Acad. Sci. U. S. A.* **99,** 13669–13674
39. Reid, R. J., Fiorani, P., Sugawara, M., and Bjornsti, M. A. (1999) *Proc. Natl. Acad. Sci. U. S. A.* **96,** 11440–11445
40. Walowsky, C., Fitzhugh, D. J., Castano, I. B., Ju, J. Y., Levin, N. A., and Christman, M. F. (1999) *J. Biol. Chem.* **274,** 7302–7308
41. Papa, F. R., Amerik, A. Y., and Hochstrasser, M. (1999) *Mol. Biol. Cell* **10,** 741–756
42. Swaminathan, S., Amerik, A. Y., and Hochstrasser, M. (1999) *Mol. Biol. Cell* **10,** 2583–2594
43. Amerik, A. Y., Nowak, J., Swaminathan, S., and Hochstrasser, M. (2000) *Mol. Biol. Cell* **11,** 3365–3380
44. Ayscough, K. R., Eby, J. J., Lila, T., Dewar, H., Kozminski, K. G., and Drubin, D. G. (1999) *Mol. Biol. Cell* **10,** 1061–1075
45. Holtzman, D. A., Yang, S., and Drubin, D. G. (1993) *J. Cell Biol.* **122,** 635–644
46. Gourlay, C. W., Dewar, H., Warren, D. T., Costa, R., Satish, N., and Ayscough, K. R. (2003) *J. Cell Sci.* **116,** 2551–2564
47. Chabes, A., Domkin, V., and Thelander, L. (1999) *J. Biol. Chem.* **274,** 36679–36683
48. Longtine, M. S., McKenzie, A., III, Demarini, D. J., Shah, N. G., Wach, A., Brachat, A., Philippsen, P., and Pringle, J. R. (1998) *Yeast* **14,** 953–961
49. Sikorski, R. S., and Hieter, P. (1989) *Genetics* **122,** 19–27
50. Schneider, B. L., Seufert, W., Steiner, B., Yang, Q. H., and Futcher, A. B. (1995) *Yeast* **11,** 1265–1274
51. Adams, A. E., and Pringle, J. R. (1991) *Methods Enzymol.* **194,** 729–731
52. Raymond, C. K., Howald-Stevenson, I., Vater, C. A., and Stevens, T. H. (1992) *Mol. Biol. Cell* **3,** 1389–1402
53. Mulholland, J., Preuss, D., Moon, A., Wong, A., Drubin, D., and Botstein, D. (1994) *J. Cell Biol.* **125,** 381–391
54. Clark, M. W. (1991) *Methods Enzymol.* **194,** 608–626
55. Byers, B., and Goetsch, L. (1991) *Methods Enzymol.* **194,** 602–608
56. Kauh, E. A., and Bjornsti, M.-A. (1995) *Proc. Natl. Acad. Sci. U. S. A.* **92,** 6299–6303
57. Bordo, D., and Bork, P. (2002) *EMBO Rep.* **3,** 741–746
58. Amerik, A. Y., Li, S. J., and Hochstrasser, M. (2000) *Biol. Chem.* **381,** 981–992
59. Tang, H. Y., Xu, J., and Cai, M. (2000) *Mol. Cell. Biol.* **20,** 12–25
60. Zou, L., Mitchell, J., and Stillman, B. (1997) *Mol. Cell. Biol.* **17,** 553–563
61. Babst, M., Katzmann, D. J., Estepa-Sabal, E. J., Meerloo, T., and Emr, S. D. (2002) *Dev. Cell* **3,** 271–282
62. Chabes, A., Georgieva, B., Domkin, V., Zhao, X., Rothstein, R., and Thelander, L. (2003) *Cell* **112,** 391–401
63. Zhao, X., Chabes, A., Domkin, V., Thelander, L., and Rothstein, R. (2001) *EMBO J.* **20,** 3544–3553
64. Melo, J., and Toczyski, D. (2002) *Curr. Opin. Cell. Biol.* **14,** 237–245
65. Nyberg, K. A., Michelson, R. J., Putnam, C. W., and Weinert, T. A. (2002) *Annu. Rev. Genet.* **36,** 617–656
66. Redon, C., Pilch, D. R., Rogakou, E. P., Orr, A. H., Lowndes, N. F., and Bonner, W. M. (2003) *EMBO Rep.* **4,** 1–7
67. Wan, S., and Walworth, N. C. (2001) *Curr. Genet.* **38,** 299–306
68. Pouliot, J. J., Yao, K. C., Robertson, C. A., and Nash, H. A. (1999) *Science* **286,** 552–555
69. Katzmann, D. J., Odorizzi, G., and Emr, S. D. (2002) *Nat. Rev. Mol. Cell. Biol.* **3,** 893–905
70. Desai, S. D., Zhang, H., Rodriguez-Bauman, A., Yang, J. M., Wu, X., Gounder, M. K., Rubin, E. H., and Liu, L. F. (2003) *Mol. Cell. Biol.* **23,** 2341–2350
71. Desai, S. D., Mao, Y., Sun, M., Li, T. K., Wu, J., and Liu, L. F. (2000) *Ann. N. Y. Acad. Sci.* **922,** 306–308
72. Peng, J., Schwartz, D., Elias, J. E., Thoreen, C. C., Cheng, D., Marsischky, G., Roelofs, J., Finley, D., and Gygi, S. P. (2003) *Nat. Biotechnol.* **21,** 921–926
73. Singer, J. D., Manning, B. M., and Formosa, T. (1996) *Mol. Cell. Biol.* **16,** 1356–1366
74. Katou, Y., Kanoh, Y., Bando, M., Noguchi, H., Tanaka, H., Ashikari, T., Sugimoto, K., and Shirahige, K. (2003) *Nature* **424,** 1078–1083
75. Osborn, A. J., and Elledge, S. J. (2003) *Genes Dev.* **17,** 1755–1767

The Deubiquitinating Enzyme Doa4p Protects Cells from DNA Topoisomerase I Poisons

Paola Fiorani, Robert J. D. Reid, Antonino Schepis, Hervé R. Jacquiau, Hong Guo, Padma Thimmaiah, Piero Benedetti and Mary-Ann Bjornsti

J. Biol. Chem. 2004, 279:21271-21281.
doi: 10.1074/jbc.M312338200 originally published online February 26, 2004
